Communicated by Paul Adams

Sensitivity of Synaptic Plasticity to the Ca^{2+} Permeability of NMDA Channels: A Model of Long-Term Potentiation in Hippocampal Neurons

Erik De Schutter
James M. Bower
Division of Biology 216-76, California Institute of Biology, Pasadena, CA 91125 USA

We have examined a model by Holmes and Levy (1990) of the induction of associative long-term potentiation (LTP) by a rise in the free Ca^{2+} concentration ($[Ca^{2+}]$) after synaptic activation of dendritic spines. The previously reported amplification of the change in $[Ca^{2+}]$ caused by coactivation of several synapses was found to be quite sensitive to changes in the permeability of the *N*-methyl-D-aspartate (NMDA) receptor channels to Ca^{2+}. Varying this parameter indicated that maximum amplification is obtained at values that are close to Ca^{2+} permeabilities reported in the literature. However, amplification failed if permeability is reduced by more than 50%. We also found that the maximum free $[Ca^{2+}]$ reached in an individual spine during synaptic coactivation of several spines depended on the location of that spine on the dendritic tree. Distal spines attained a higher $[Ca^{2+}]$ than proximal ones, with differences of up to 80%. The implications of this result for the uniformity of induction of associative LTP in spines in different regions of the dendrite are discussed.

1 Introduction

Since Hebb (1949) first proposed that a synaptic modification based on the co-occurrence of pre- and postsynaptic activity might underlie learning, this idea has formed the basis for many models of network associative learning (Byrne and Berry 1989). Over the last decade, neurobiologists have been studying a physiological phenomenon known as long-term potentiation (LTP), which can have many of the associative properties on synaptic strengths that Hebb originally hypothesized (Nicoll *et al.* 1988). Recent work in the hippocampus has implicated a particular membrane channel, the *N*-methyl-D-aspartate (NMDA) receptor channel, in a type of LTP that is clearly associative (Landfield and Deadwyler 1988). In this case, an increase in synaptic strength is induced when synaptic stimulation coincides with depolarization of the postsynaptic membrane. The

dependence on postsynaptic depolarization appears to rely on the release of a voltage dependent block of this channel by Mg^{2+} ions (Mayer *et al.* 1984; Nowak *et al.* 1984; Ascher and Nowak 1988). When this block is released, binding of glutamate to the NMDA channel causes an influx of Ca^{2+}, a rise in free $[Ca^{2+}]$ in the dendritic spine (Regehr and Tank 1990; Müller and Connor 1991), and a change in synaptic efficacy by an as yet not understood secondary mechanism.

NMDA channels are permeable to Na^+ and K^+ as well as to Ca^{2+} (Mayer and Westbrook 1987; Ascher and Nowak 1988). In most experimental studies on LTP total ionic current through the NMDA channel is measured. The Ca^{2+} influx is only a small fraction of this total current and it is usually not measured separately, despite its crucial role in the induction of LTP. This distinction may be important because it is known that the Ca^{2+} permeability of other glutamate receptor channels can vary depending on the subunit composition of the channel receptor complex (Hollmann *et al.* 1991).

The apparent association between LTP and conditions for associative memory (Landfield and Deadwyler 1988) has made LTP the subject of a growing number of modeling efforts (Gamble and Koch 1987; Holmes and Levy 1990; Zador *et al.* 1990). Given its putative role in actually triggering the induction of a synaptic change, the Ca^{2+} influx and the rise in the cytoplasmic Ca^{2+} concentration ($[Ca^{2+}]$) in the dendritic spine have been a central focus of this work. Holmes and Levy (1990) have used their modeling results to argue that the simple influx of Ca^{2+} alone is not enough to account for associative effects. Instead they stated that associative LTP could be controlled by a steep nonlinearity in the relation between $[Ca^{2+}]$ and the number of coactivated synapses. To show this relation, they used an anatomically reconstructed hippocampal dentate granule cell to build a structurally realistic model (HL model) that included NMDA and non-NMDA receptors on dendritic spines, Ca^{2+} diffusion, a Ca^{2+} buffer, and a pump. With this model they demonstrated that while the Ca^{2+} influx increases only moderately if a large number of synapses are coactivated, the resulting internal free $[Ca^{2+}]$ can increase 20- to 30-fold.

To make their case Holmes and Levy explored several of the important parameters of their model. For example, they demonstrated that the amplification result was robust for changes in Ca^{2+} buffer binding characteristics and buffer concentrations. However, they did not examine the dependence of their results on the Ca^{2+} permeability of the NMDA channel.

In this paper we have explored the consequences of changing the Ca^{2+} permeability, that is, changing the size of the Ca^{2+} influx for a given NMDA-current. We have reconstructed the original HL model within the GENESIS simulation environment and have replicated the previously published results. In addition, we have shown that the maximum free $[Ca^{2+}]$ after NMDA channel coactivation is actually quite sensitive to

the Ca^{2+} permeability. We have also demonstrated that there may be a considerable difference in the peak $[Ca^{2+}]$ expected in spines located in different regions of the dendrite. This result reinforces the idea that the induction of LTP does not only depend on the properties of the NMDA channel and of the Ca^{2+} buffers, but also on the electrical structure of the postsynaptic neuron.

2 Implementation of the Holmes–Levy Model in GENESIS

The HL model was ported to the Caltech neuronal simulation system, GENESIS (Wilson *et al.* 1989). Two major changes were made to the model. The compartmental structure of the model was simplified to reduce the computational overhead and the equations for the conductance of NMDA and non-NMDA channels were changed to a standard type (Perkel *et al.* 1981).

We modeled 98 dendritic spines, each with 7 compartments representing a cylindrical head of 0.55 by 0.55 μm on a neck of 0.10 by 0.73 μm (Fig. 3 of HL). Each compartment in the spine contained a calcium buffer (100 μM, 200 μM at the top of the head), a Ca^{2+} pump and Ca^{2+} could diffuse between spine compartments and into the neighboring dendrite.

At the top of the spine head NMDA and non-NMDA channels were located. In contrast to the HL model, a standard reaction scheme (Perkel *et al.* 1981) implemented in GENESIS was used for the NMDA and non-NMDA conductance:

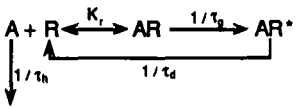

(2.1)

A is the transmitter, *R* the receptor, *AR* the closed transmitter-receptor complex, and *AR** the open transmitter-receptor complex. The original HL model used two variants of the reaction scheme leading to *AR**. In the current model the rate factors in equation 2.1 have been optimized to give the same values of *AR** as the HL model (cf. their Fig. 4). Because the value of *AR** is the only variable directly relevant to the modeling conclusions, these differences in the reaction scheme are not pertinent. Values used for the non-NMDA channel were τ_g 600 msec, τ_h 1.25 msec, τ_d 0.001 msec, K_r 2 μM, $g = 5$ pS. For the NMDA channel τ_g 283 sec, τ_h 5.88 msec, τ_d 0.002 msec, K_r 50 μM, $g = 50$ pS.

Equations for the voltage-dependent Mg^{2+} block of NMDA channels and for Ca^{2+} diffusion, buffers, and pumps were identical to those in the HL model. The fraction of NMDA current carried by Ca^{2+} was based on the permeabilities to Ca^{2+}, Na^+, and K^+ of NMDA channels (Goldman equations of Mayer and Westbrook 1987). Figure 1 shows that within the voltage and $[Ca^{2+}]$ ranges used in the model, only voltage changed this fraction. Because Ca^{2+} inflow was computed as a fraction of total

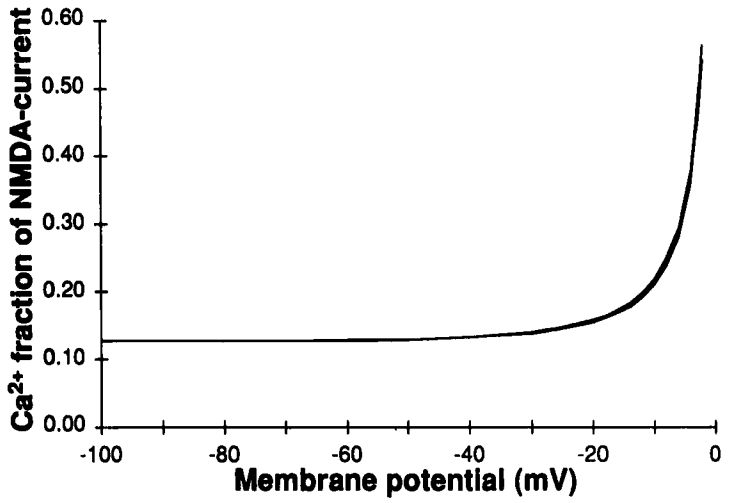

Figure 1: Dependence of the fraction of total NMDA current carried by Ca^{2+} on membrane potential for five different concentrations of internal $[Ca^{2+}]$ (0.02, 0.20, 2.00, 20, and 200 μM) at an external $[Ca^{2+}]$ of 2 mM. Because total NMDA current becomes zero around 0 mV (the reversal potential), the solution becomes asymptotic close to this potential. Note that most of the curves overlap, only at internal Ca^{2+} concentrations above 100 μM does internal $[Ca^{2+}]$ affect this fraction.

NMDA current, there was no need compute the Ca^{2+} Nernst potential. The reversal potential of the NMDA current itself changed by less than 0.1 mV for a change in internal $[Ca^{2+}]$ from 20 nM to 2 mM (which is the external $[Ca^{2+}]$).

The total number of compartments in the model was 1192. The same cable parameters were used as in the HL model. The spines were randomly distributed over two 165-μm-long dendritic segments, which each contained 98 dendritic spines (inset in Fig. 4). The rest of the compartmental model was highly simplified, having only 20 compartments that represented the soma and 5 other dendrites. This simplification was possible because, under conditions where the active spines are the only source of depolarizing currents, the soma and other dendrites act only as a current drain. Accordingly, as long as the passive load corresponding to the soma and these dendrites was correct, a simplified model produces the same results for the dendritic spines as a detailed model. The input resistance at the soma was 74.4 MΩ, compared to 72.4 MΩ in the HL model.

To quantify model results, relative Ca^{2+} permeability was defined as the ratio between the value used in a particular simulation and the Ca^{2+} permeability reported by Mayer and Westbrook (1987). A relative Ca^{2+} permeability of one was thus the experimental value, which corresponded to 12.8% of the NMDA current at −70 mV being carried by Ca^{2+} ions (Fig. 1).

We have adopted the same definition of amplification ratio as introduced by HL, that is, the ratio between maximum free $[Ca^{2+}]$ in a particular spine after coactivation of 96 synapses over the maximum free $[Ca^{2+}]$ after activation of the synapse on that single spine. The stimulus paradigm for induction of LTP was 8 pulses at 200 Hz as in HL.

The GENESIS implementation of the HL model described in this paper can be obtained by ftp from babel.cns.caltech.edu.

3 Results

In general, our implementation of the HL model within the GENESIS simulation software gave qualitatively equivalent results to those reported by Holmes and Levy. The change in membrane potential and NMDA channel conductance in two dendritic spines during coactivation of 96 spines is compared in Figure 2 with the original data from HL (their Fig. 7). The small differences in peak values were probably caused by sampling, because the size of the responses to synaptic activation was different in every spine. Because we implemented the same Ca^{2+} mechanisms as employed in the HL model, our model also reproduced their computations of $[Ca^{2+}]$ exactly (results not shown).

The main new modeling results are presented in Figure 3. Figure 3A shows the sharp dependency of the amplification ratio on the relative Ca^{2+} permeability of the NMDA channel. For 96 coactivated spines versus 1 spine, under the standard conditions of the HL model, the amplification curve peaked at a relative permeability of about 1.25. At lower permeabilities the amplification ratio declined steeply and it dropped below 5 at a relative permeability of 0.50. At higher permeabilities it slowly declined to an amplification ratio of about 10. This dependency was similar for all dendritic spines, independent of their location; there was only a difference in amplitude.

The relation between maximum free $[Ca^{2+}]$ and relative Ca^{2+} permeability was shallow and nonlinear for low permeabilities, and steeper and linear for higher permeabilities (Fig. 3B). A peak appeared in the amplification ratio to permeability curve because the linear part started at lower permeability values for activation of 96 spines than for 1 spine.

We also examined the effect of changing important parameters in the HL model on the amplification ratio to permeability curve. Changes in the buffer concentration in the spine head changed the location and size of the peak, but not the general shape of the curve (Fig. 3C). For lower

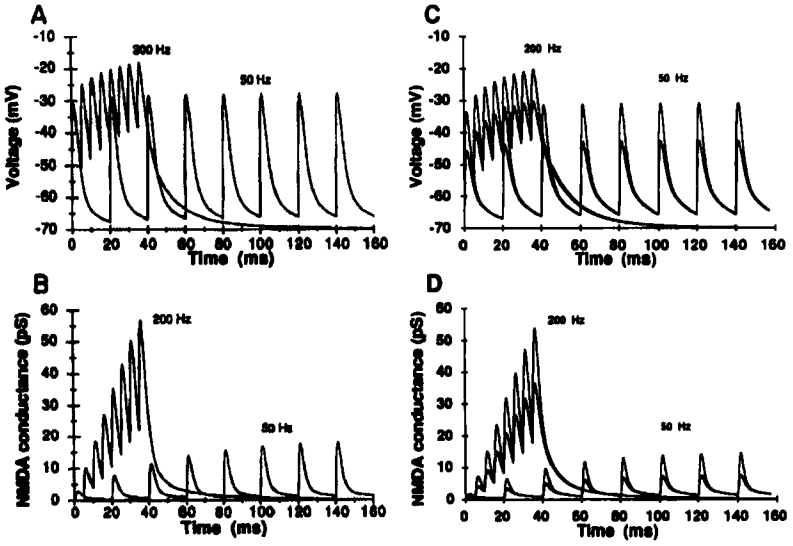

Figure 2: Spine head membrane potential and NMDA receptor-mediated synaptic conductance for two different spines during coactivation of 96 spine synapses at 50 and 200 Hz. A and B are the original figures of Holmes and Levy (1990, courtesy of The American Physiological Society) and C and D are the corresponding figures produced by the implementation of their model described in this report. In C and D the responses in a distal spine (upper lines) and a proximal spine are shown. The responses in the distal spine are always bigger than in the proximal one. (A, C) Membrane potential as a function of time. (B, D) NMDA channel conductance at the synapse on the same spine heads. Proximal spine is spine #1, distal spine is spine #6 (see Fig. 4).

buffer concentrations the peak was smaller and occurred at smaller relative Ca^{2+} permeabilities. The reverse was true for higher buffer concentrations.

Changes of the rate constant of the calcium pump by a factor of 2 did not change the amplification ratio versus permeability curve and changed the maximum free $[Ca^{2+}]$ by less than 1% (results not shown).

We found the amplification ratio to permeability curve to be quite sensitive to the amount of transmitter released presynaptically (A in equation 2.1), which would affect both the NMDA- and non-NMDA-mediated components of the postsynaptic response (Fig. 3D). Doubling the amount of transmitter released per stimulus sharpened the peak considerably and shifted it to low relative Ca^{2+} permeability values (peaking at about 0.5).

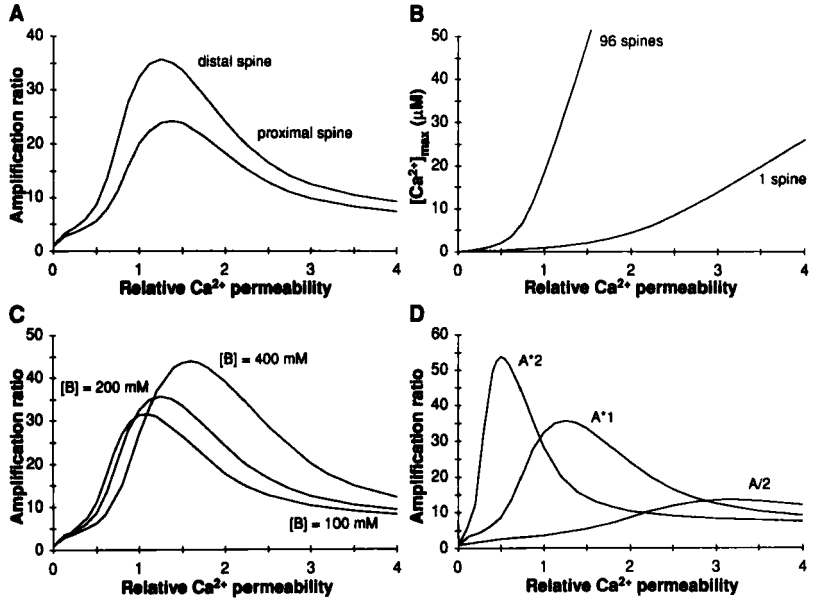

Figure 3: Amplification ratio after a 200 Hz stimulus as a function of relative Ca^{2+} permeability under different model conditions. (A) Standard HL model amplification at two different spines, located distally (upper line, spine 6 in Fig. 4) and proximally on the dendrite (spine 1 Fig. in 4), is compared. (B) Maximum $[Ca^{2+}]$ as a function of relative Ca^{2+} permeability after activation of 1 or 96 spines in the proximal spine. (C) Effect of changing buffer concentration [B] in the spine head on the amplification ratio. (D) Effect of changing the amount of transmitter released per stimulus (A) on the amplification ratio.

Halving the transmitter release flattened the curve so that no clear peak could be distinguished; it also greatly diminished the amplification ratio at all levels of Ca^{2+} permeability.

As our results suggested a big variation in amplification ratios between different spines, we compared the time course of $[Ca^{2+}]$ for spines located on different parts of the dendritic tree (Fig. 4). Because of the passive electrical properties of dendrites, distal regions of the cell were likely to be more depolarized than proximal regions for the same amount of input (Fig. 2C). This was a consequence of the passive load of the soma and other dendrites on proximal regions. This in turn means that NMDA channels on distal spines were less blocked by Mg^{2+} than channels in proximal spines (Fig. 2D). As a result, the Ca^{2+} concentration reached peaks in distal spines that were 20 to 80% higher than in proximal spines. Further, because there was very little difference in maximum free $[Ca^{2+}]$ after activation of a single synapse (2 to 3%, depending on the relative

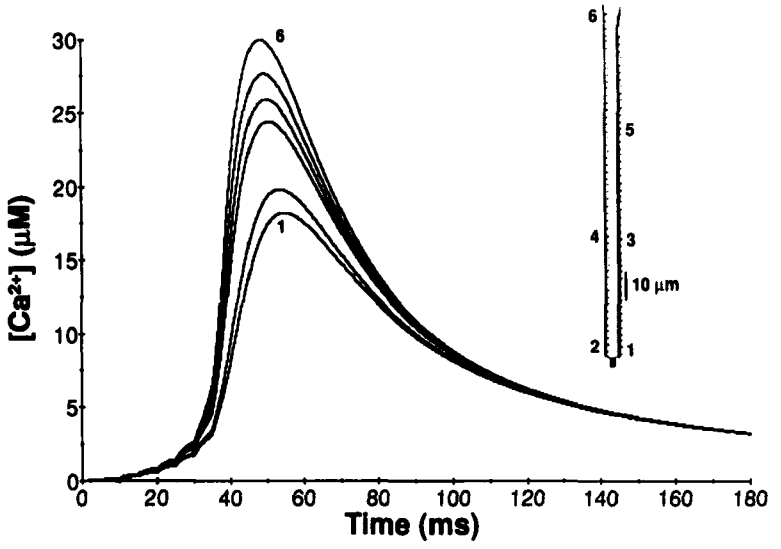

Figure 4: Calcium concentration as a function of time in six spines at different dendritic locations during coactivation of 96 spines. The location of the spines is shown on the gray schematic at the upper right; the six spines are shown in black.

Ca^{2+} permeability), differences in amplification ratio also varied between 20 and 80% (Fig. 2). This effect was most pronounced for relative Ca^{2+} permeabilities of 0.5 to 1.5, which straddle reported experimental values.

Within spine heads, there was almost no gradient of free Ca^{2+} or free buffer. For example, 18 msec after the last stimulus at 200 Hz, when free $[Ca^{2+}]$ reached its peak value, $[Ca^{2+}]$ was 30.20 μM under the membrane and 29.37 μM at the base of the spine head. There was however a big gradient over the spine neck, as $[Ca^{2+}]$ in the underlying dendritic shaft was only 0.09 μM.

4 Discussion

In this paper we have extended the examination of the parameter space in a previously published biophysical model of associative LTP (Holmes and Levy 1990). While this is the most detailed model of $[Ca^{2+}]$ changes during activation of NMDA receptors on dendritic spines published to date, other models of LTP related changes in $[Ca^{2+}]$ have been reported. For ex-

ample, an older model by Gamble and Koch (1987) predicted changes in internal calcium concentrations during LTP. However, this model did not explicitly make use of NMDA channels. A second, more recent model by Zador *et al.* (1990) has essentially the same components as the HL model, but simulates only one spine on a compartmental model of a pyramidal cell and uses a fixed Ca^{2+} permeability that is independent of voltage (compare to Fig. 1). We expect that the changes in relative Ca^{2+} permeability described here would have a similar effect in this model. Other models of LTP (Kitajima and Hara 1990) or NMDA channels (Jahr and Stevens 1990) were not constructed to simulate realistic changes in $[Ca^{2+}]$.

The principal results described here are the apparent sensitivity of the Holmes and Levy model to the Ca^{2+} permeability of the NMDA channel and to the dendritic position of the activated spines. These properties were a direct consequence of the $[Ca^{2+}]$ amplification mechanism on which the HL model is based, that is, buffer saturation in the spine head. Optimal amplification happened when most of the inflowing Ca^{2+} was bound to buffers after a single spine was activated, while coactivation of many spines saturated buffers completely and caused consequently a large rise in free $[Ca^{2+}]$. The buffers in the spine head could saturate, because diffusion out of the spine was restricted as shown by the large drop in $[Ca^{2+}]$ over the spine neck. The HL model fits within present theories of the physiological function of dendritic spines, which emphasize the compartmentalization of chemical processes in the spine head (Koch *et al.* 1992).

It has been shown in large cells that diffusion of Ca^{2+} buffers may have a profound effect on dynamic changes in $[Ca^{2+}]$ (Sala and Hernández-Cruz 1990). The HL model does not simulate diffusion of buffers, but based on our results we do not think that such diffusion plays any role in this system. Because of the small volume of the spine head, there was almost no gradient of free or bound Ca^{2+} buffers. There was a big gradient over the spine neck, but presumably buffers would diffuse much slower through this restricted space than Ca^{2+} itself.

The interaction between buffer saturation and relative Ca^{2+} permeability of the NMDA channel produced several interesting results, some of which may be counterintuitive. For example, increasing the amplitude of the synaptic conductance actually decreased the sensitivity of the system to distinguish between activation of a few or a lot of spines. This was evidenced by the small drop in amplification ratio at a relative permeability of 1.0 (Fig. 3D). If synaptic conductance was increased even more, the decrease would have become more pronounced. Decreasing the synaptic conductance was worse, because the amplification ratio dropped below 5. These results are important as both a short-term and long-term potentiation and a depression of synaptic conductance have been described at hippocampal synapses (Larkman *et al.* 1991; Malenka 1991).

Surprisingly, changing the amount of buffer in the spine head had much less effect on the amplification ratio at a relative Ca^{2+} permeability

of 1.0 (Fig. 3C), as was also pointed out by Holmes and Levy. At higher relative Ca^{2+} permeabilities, higher buffer concentrations increased the sensitivity of the system. Note that decreasing the buffer concentration could not fully compensate for large decreases in Ca^{2+} permeability.

It has not been proven that a nonlinear amplification of $[Ca^{2+}]$ is the critical feature in associative LTP. For example, if the next step in the induction of LTP (e.g., activation of a Ca^{2+}-dependent kinase; Miller and Kennedy 1986) has a sharp, nonlinear dependence on $[Ca^{2+}]$, then such a mechanism might be robust enough to operate with smaller changes in $[Ca^{2+}]$ (Zador et al. 1990). However, recent imaging experiments do show increases in $[Ca^{2+}]$ from a resting level of 0.05 to 1.30 μM in dendritic spines under conditions that are expected to induce LTP (Müller and Connor 1991). Holmes and Levy argue that the nonlinearity underlying the induction of associative LTP should be as steep as possible and they eliminate Ca^{2+} influx itself as a potential inductor because it is amplified by a factor of only 3. Combining this argument with the experimental data, it seems reasonable to assume that a safe amplification factor for the induction of associative LTP should be at least 10.

Thus, we have shown that diminishing the Ca^{2+} permeability by 50% makes the amplification ratio too small to function as a reliable inductor of associative LTP. The same is true for a decrease in the synaptic conductance. Increasing the Ca^{2+} permeability changed the amplification ratio also, but it never dropped below 10. Holmes and Levy did not report the effects of changing these critical model parameters on the predictions made by their model.

We have also shown that the location of a particular dendritic spine with respect to the electrical structure of the entire cell may have a profound effect on its participation in LTP. Our results suggest that LTP may be a cooperative phenomenon that besides nonlinear interaction between NMDA channels also involves the structure of the entire postsynaptic neuron. The interaction of Ca^{2+} effects with the passive electrical properties of the cell's dendrite could result in changes of the amplification ratio of up to 80% depending on the particular position of a spine. Whether the difference between a peak $[Ca^{2+}]$ of 18.5 versus 29.8 μM (Fig. 4) would also cause quantitative differences in the amount of LTP induced is unknown at present. This can be determined only after more experimental data have become available, so that biochemical models of the processes involved in LTP induction can be developed.

The current simulations have examined the somewhat unlikely occurrence of activation in only two dendritic segments. Similar effects could be produced if network circuitry results in differential activation and/or inhibition of different regions of a particular dendrite. In this regard, our network simulations of the olfactory piriform cortex (Wilson and Bower 1992) and neocortex (Wilson and Bower 1991) make it seem quite likely that the laminar organization of both the cortex and the hippocampus (Brown and Zador 1990) could easily produce such differential effects

on pyramidal cells. In this context, Mel (1992) reported that a modeled cortical pyramidal neuron with NMDA channels responds preferentially to clustered synaptic inputs versus distributed ones. Location-dependent differences in the magnitude of LTP have been reported in the piriform cortex by Kanter and Haberly (1990). They reported, however, an inverse relation to what the model predicts, that is, LTP induced by association fibers on the proximal parts of the dendrite was larger than that induced by the more distally located afferent fibers. This discrepancy can be explained by several factors, among them specific differences in the NMDA receptors themselves (see further) and the effect of somatic action potentials, which would depolarize proximal NMDA channels more than distal ones (and thus remove the effect of the voltage-dependent Mg^{2+} block).

There are several possible consequences of such a location dependence. It is conceivable, for example, that variations in amplification effects in dendritic regions could reflect functional differences in projecting fiber systems. It may be that the operation of a particular neuron would depend on excluding synapses in certain positions from participating in LTP even in the presence of NMDA receptors. For example, there are several examples known where NMDA receptors are present but LTP has not been demonstrated (Artola and Singer 1987). In this case the electrical properties of some neurons may not support the amplification effects shown in the HL model. As pointed out above, in other cases spread of somatic action potentials into the proximal parts of the dendritic tree might counteract the location dependence.

While it is interesting to speculate on the possible effects of cell structure and changes in presynaptic transmitter release on the induction of associative LTP, there are ways in which the effects we have described could be overcome. For example position-dependent changes in Ca^{2+} conductivity could counteract the effects shown here. This could be achieved by changing the ratio of NMDA versus non-NMDA receptors or by changing the Ca^{2+} permeability of the NMDA channel. In this regard, recent reports of the permeability to cations of reconstituted non-NMDA channels show that permeability can vary with the subunit composition of the channel complex (Hollmann *et al.* 1991). It has also been shown that the expression of non-NMDA channel subunits that make the channel permeable to Ca^{2+} can be tissue and cell specific (Burnashev *et al.* 1992). Though subunit specific variability in cation permeability has not been shown for the NMDA channel, it suggests a molecular mechanism for creating localized differences in Ca^{2+} permeability. Bekkers and Stevens (1990) report significantly lower Ca^{2+} permeabilities for NMDA channels in hippocampal neurons, compared to the values determined by Mayer and Westbrook (1987) in mouse spinal cord neurons (respectively, 4.5 or 12.8% of the NMDA current being carried by Ca^{2+} at 2 mM external $[Ca^{2+}]$). It is also conceivable that the Ca^{2+} permeability of the NMDA channel might be affected by phosphorylation of the channel proteins. Similar changes in the degree of phosphorylation have been implicated

in numerous molecular mechanisms presumed to be involved in synaptic function (Huganir and Greengard 1990) and protein kinase C has been shown to potentiate NMDA current by reducing the voltage-dependent Mg^{2+} block (Ben-Ari *et al.* 1992). Changing specifically the Ca^{2+} permeability of NMDA channels, while keeping their density and total conductance unchanged, would have the advantage that the induction of LTP could be controlled without changing the electrical properties of the neuron.

Finally, whatever the significance of differences in dendritic location, our modeling results draw attention to the critical question of the actual permeabilities of NMDA channels to Ca^{2+}. Mayer and Westbrook (1987) and Ascher and Nowak (1988) have pointed out that Goldman (1943) equations (used in the HL model) cannot account for the full properties of the NMDA channel. It is interesting to note that the experimental values for Ca^{2+} permeability reported by Mayer and Westbrook (1987) are within 25% of the values that cause a maximum amplification of free $[Ca^{2+}]$ in the spine head in the HL model. Assuming that other parameters of the model are accurate, this suggests that the dendritic spine apparatus and its control over $[Ca^{2+}]$ may operate close to maximal efficiency for sensing coactivation of synapses. However, this would not be true for the Ca^{2+} permeabilities reported by Bekkers and Stevens (1990), which at a relative permeability of 0.35 correspond to an amplification of only 4 to 5. In light of the potentially profound effect on LTP of NMDA receptor permeabilities, it appears to be important to make additional measurements of this value in other brain regions showing associative LTP.

Acknowledgments

This work was supported by Fogarty fellowship F05 TW04368 to EDS and a grant from the Office of Naval Research, Contract N00014-91-5-1831. We thank the editors for useful comments on a first draft of this paper.

References

Artola, A., and Singer, W. 1987. Long term potentiation and NMDA receptors in rat visual cortex. *Nature (London)* **330**, 84–86.

Ascher, P., and Nowak, L. 1988. The role of divalent cations in the N-methyl-D-aspartate responses of mouse central neurones in culture. *J. Physiol.* **399**, 247–266.

Bekkers, J. M., and Stevens, C. F. 1990. Computational implications of NMDA receptor channels. *C.S.H. Symp. Quant. Biol.* **55**, 131–135.

Ben-Ari, Y., Anikstejn, L., and Bregestovski, P. 1992. Protein kinase C modulation of NMDA currents: An important link for LTP induction. *Trends Neurosci.* **15**, 333–339.

Brown, T. H., and Zador, A. M. 1990. Hippocampus. In *The Synaptic Organization of the Brain*, G. M. Shepherd, ed., pp. 346–388. Oxford University Press, New York.

Burnashev, N., Khodorova, A., Jonas, P., Helm, P. J., Wisden, W., Monyer, H., Seeburg, P. H., and Sakmann, B. 1992. Calcium-permeable AMPA-kainate receptors in fusiform cerebellar glial cells. *Science* **256**, 1566–1570.

Byrne, J. H., and Berry, W. O., eds. 1989. *Neural Networks of Plasticity: Experimental and Theoretical Approaches.* Academic Press, San Diego.

Gamble, E., and Koch, C. 1987. The dynamics of free calcium in dendritic spines in response to repetitive synaptic input. *Science* **236**, 1311–1315.

Goldman, D. E. 1943. Potential, impedance, and rectification in membranes. *J. Gen. Physiol.* **27**, 37–60.

Hebb, D. O. 1949. *The Organization of Behavior: A Neuropsychological Theory.* John Wiley, New York.

Hollmann, M., Hartley, M., and Heinemann, S. 1991. Ca^{2+} permeability of KA-AMPA-gated glutamate receptor channels depends on subunit composition. *Science* **252**, 851–853.

Holmes, W. R., and Levy, W. B. 1990. Insights into associative long-term potentiation from computational models of NMDA receptor-mediated calcium influx and intracellular calcium concentration changes. *J. Neurophysiol.* **63**, 1148–1168.

Huganir, R. L., and Greengard, P. 1990. Regulation of neurotransmitter receptor desensitization by protein phosphorylation. *Neuron* **5**, 555–567.

Jahr, C. E., and Stevens, C. F. 1990. Voltage dependence of NMDA-activated macroscopic conductances predicted by single-channel kinetics. *J. Neurosci.* **10**, 3178–3182.

Kanter, E. D., and Haberly, L. B. 1990. NMDA-dependent induction of long-term potentiation in afferent and association fiber systems of piriform cortex *in vitro*. *Brain Res.* **525**, 175–179.

Kitajima, T., and Hara, K. 1990. A model of the mechanisms of long-term potentiation in the hippocampus. *Biol. Cybern.* **64**, 33–39.

Koch, C., Zador, A., and Brown, T. H. 1992. Dendritic spines: Convergence of theory and experiment. *Science* **256**, 973–974.

Landfield, P. W., and Deadwyler, S. A., eds. 1988. *Long-term Potentiation: From Biophysics to Behavior.* Alan Liss, New York.

Larkman, A., Stratford, K., and Jack, J. 1991. Quantal analysis of excitatory synaptic action and depression in hippocampal slices. *Nature (London)* **350**, 344–347.

Malenka, R. C. 1991. Postsynaptic factors control the duration of synaptic enhancement in area CA1 of the hippocampus. *Neuron* **6**, 53–60.

Mayer, M. L., and Westbrook, G. L. 1987. Permeation and block of N-methyl-D-aspartic acid receptor channels by divalent cations in mouse cultured central neurones. *J. Physiol. London* **394**, 501–527.

Mayer, M. L., Westbrook, G. L., and Guthrie, P. B. 1984. Voltage-dependent block

by Mg^{2+} of NMDA-responses in spinal cord neurones. *Nature (London)* **309**, 261–263.

Mel, B. 1992. NMDA-based pattern discrimination in a modeled cortical neuron. *Neural Comp.* **4**, 502–517.

Miller, S. G., and Kennedy, M. B. 1986. Regulation of brain type II Ca^{2+}/calmodulin-dependent protein kinase by autophosphorylation: A Ca^{2+}-triggered molecular switch. *Cell* **44**, 861–870.

Müller, W., and Connor, J. A. 1991. Dendritic spines as individual neuronal compartments for synaptic Ca^{2+} responses. *Nature (London)* **354**, 73–76.

Nicoll, R. A., Kauer, J. A., and Malenka, R. C. 1988. The current excitement in long-term potentiation. *Neuron* **1**, 97–103.

Nowak, L., Bregestovski, P., Ascher, P., Herbert, A., and Prochiantz, A. 1984. Magnesium gates glutamate-activated channels in mouse central neurones. *Nature (London)* **307**, 462–465.

Perkel, D. H., Mulloney, B., and Budelli, R. W. 1981. Quantitative methods for predicting neuronal behavior. *Neuroscience* **4**, 823–837.

Regehr, W. G., and Tank, D. W. 1990. Postsynaptic NMDA receptor-mediated calcium accumulation in hippocampal CA1 pyramidal cell dendrites. *Nature (London)* **345**, 807–810.

Sala, F., and Hernández-Cruz, A. 1990. Calcium diffusion modeling in a spherical neuron. Relevance of buffering properties. *Biophys. J.* **57**, 313–324.

Wilson, M. A., and Bower, J. M. 1991. A computer simulation of oscillatory behavior in primary visual cortex. *Neural Comp.* **3**, 498–509.

Wilson, M. A., and Bower, J. M. 1992. Cortical oscillations and temporal interactions in a computer simulation of piriform cortex. *J. Neurophysiol.* **67**, 981–995.

Wilson, M. A., Bhalla, U. S., Uhley, J. D., and Bower, J. M. 1989. GENESIS: A system for simulating neural networks. In *Advances in Neural Information Processing Systems*, D. Touretzky, ed., pp. 485–492. Morgan Kaufmann, San Mateo, CA.

Zador, A., Koch, C., and Brown, T. H. 1990. Biophysical model of a Hebbian synapse. *Proc. Natl. Acad. Sci. U.S.A.* **87**, 6718–6722.

Received 20 March 1992; accepted 25 January 1993.